Hydroxyapatite Powder Prepared by Low Temperature Hydrothermal Method from Sea Shells

Ahmad Fadli*, Fajril Akbar, Pancasila Putri, Dewi Indah Pratiwi and Ikhbal Muhara

Department of Chemical Engineering, Faculty of Engineering, University of Riau Kampus Binawidya Jl. HR Subrantas Km. 12,5 Pekanbaru 28293 Riau Indonesia

*Corresponding author: fadliunri@yahoo.com

Paper History

Received: 25-October-2014 Accepted: 13-November-2014

ABSTRACT

Hydroxyapatite is bioceramics that widely used in the medical world especially for bone implant and cell culture. Hydroxyapatite was synthesized by low temperature hydrothermal method which sea shells as derived CaO and (NH₄)₂HPO₄ with Ca/P ratio of 0.67, 1.67, 2.67 were heated at 70°C, 80°C, 90°C and stirred at 300 rpm. The obtained paste was dried and then the powder calcined in the temperature range of 700°C - 1000°C. In order to study the morphology and structural characteristics, XRD and SEM were used to estimate the particle size of the powder. FTIR was used to identify organic or inorganic chemicals for estimating the number of components of an unknown mixture. The crystal diameter of hydroxyapatite increased with Ca/P ratio and reaction temperature. Majority hydroxyapatite phase was obtained at Ca/P ratio of 2.67 and 90°C reaction temperature.

KEY WORDS: Hydroxiapatite, hydrothermal, powder, characterization

1.0 INTRODUCTION

Hydroxyapatite (HAP) is the main mineral constituent of teeth and bones [1]. Because of bicompatibility, bioactivity, low solubility in water and ability to replace toxic ions, HAP $(Ca_{10}(PO_4)_6(OH)_2)$ are widely used in biomaterials [2, 3]. Therefore, multiple techniques has been used for preparation of

HAP, including precipitation [4], mechanochemical [5, 6], and hydrothermal [7, 8].

As proposed by Alqap and Sopyan [9], low temperature hydrothermal method provides advantages in comparison other methods due the stable phase of HAP. It poses more convenient method for synthesis HAP with low temperature hydrothermal method than hydrothermal method because it has no need for high temperatures when forming the HAP powder, thus lowering energy costs [10]. It is also more convenient than mechanochemical procedure since low temperature hydrothermal method presents an aqueous phase that is not available in the mechanochemical method. This aqueous phase can accelerate kinetic processes that commonly limit the rate of reaction, such as dissolution, diffusion, adsorption, reaction, and crystallization [11]. The low temperature hydrothermal method also offers variability in particle size by changing the controlled variables such as temperature, pH, rate of stirring, and amount of reactants or Ca/P ratio.

2.0 EXPERIMENTAL

2.1 Materials Preparation

The starting materials in this experiment were ammonium dihydrogen phosphate ((NH₄)H₂PO₄) (Merck, Germany) and sea shell (*Anandara Granosa*) from Pekanbaru local market. Initially, sea shell were cleaned and dried at ambient temperature for 24 hours. Subsequently, dried sea shell was crushed and sieved using a 100-mesh sieve. Sea shells powder were calcinated at 1000°C for 24 hours to changed CaCO₃ to CaO, by these following reaction:

$$CaCO_3 \longrightarrow CaO + CO_2$$
 (1)

2.2 Synthesis of Hydroxyapatite Powder

For the preparation of the solution, CaO and ((NH₄)H₂PO₄ was dropwise in 600 mL distilled water with Ca/P ratio of 0.67, 1.67 and 2.67. The suspension was heated at 70°C, 80°C, 90°C while

stirred at 300 rpm until paste was obtained. Then the paste was dried at 120°C for 15 hours and crushed until powder form. The prepared powders were then calcined in furnace at 900°C. A heating rate of 5°C min⁻¹ was applied until the required temperature was reached and then the heating was continued for 1 hour. Variables in this work were Ca/P ratio (0.67, 1.67 and 2.67) and reaction temperatures (70°C, 80°C and 90°C).

2.3 Characterization

The crystal and phase structures of the samples were identified using a X-ray diffractometer (XRD) with $CuK\alpha$ (λ = 1.5418 Å) incident radiation over the 20 range of 20-60° at room temperature. Moreover, the isolate peaks assigned to (002), (112), and (300) planes were used to estimate the crystallite size (D) of HAP phases, respectively, using the well-known Scherrer's formula as followed [12]:

$$\mathbf{D} = \frac{\mathbf{k}\lambda}{6 \times \mathbf{Cos}\theta} \tag{2}$$

Where k is a shape factor equal to 0.9, λ is the X-ray wave length, β is the full-width at half-maximum (in radians), and θ is the diffraction angle related to the diffraction peak under consideration.

Fourier transform infrared spectroscopy (FTIR) was used for identification of functional groups present in the HAP powder. The morphology and size of the nanoparticles were studied using scanning electron microscopy (SEM)

3.0 RESULTS AND DISCUSSION

3.1 FTIR Spectra

FTIR spectroscopy analysis was also used in this study. FTIR identify the functional groups in the sample. Functional groups that are identified in the FTIR analysis, among others PO₄³⁻, OH, HPO₄²⁻ and CO₃²⁻ in the range 4000 to 600 cm-1 as shown in Figure 1. According Alqap and Sopyan [9] group PO₄ bands appear at wavelengths from 1100 to 1019, 958, 962 and 605 cm⁻¹ in addition to that. In 0.67 Ca/P ratio sample PO₄³⁻ ribbon appears at a wavelength of 953, 1027, and 1067 cm⁻¹. In 1.67 Ca/P ratio sample appears at a wavelength of 962, 1087, 1023 cm⁻¹, whereas in 2.67 Ca/P ratio sample at wavelengths of 963, 1024, and 1086 cm⁻¹ as shown in Figure 1.

In addition PO₄³⁻ group, there are OH⁻ ion appears by FTIR analysis of the samples. Where OH ion occurs at a wavelength of 3700 - 2500, 630, and 667 cm⁻¹. In 0.67 Ca/P ratio sample OH group appears at a wavelength of 683 and 612 cm⁻¹. In 1.67 Ca/P ratio sample appears at wavelengths 3572, 3642, 628 cm⁻¹, where as in 2.67 Ca/P ratio sample at a wavelength of 3643 and 630 cm⁻¹. Then there HPO₄²⁻ group contained at wavelengths 1308 and 1260 cm⁻¹ in 0.67 Ca/P ratio sample. Figure 1 also shows clusters at wavelengths 788 and 710 cm⁻¹ which is based on research Alqap and Sopyan [9] at the around that wavelength the functional group that appears was a group of P₂O₇. This proves the presence of calcium pyrophosphate phase.

The results obtained spectrum for each researcher of HAP is different but still in the adjacent values. The results show that there is another group of compounds that should not exist in a

pure hydroxyapatite. Figure 2 shows the FTIR spectrum of synthesized hydroxyapatite with variations in temperature 70°C, 80°C and 90°C. The measurement results of hydroxyapatite synthesized using hydrothermal method with temperature at 70°C using FTIR analysis shown in Figure 2.

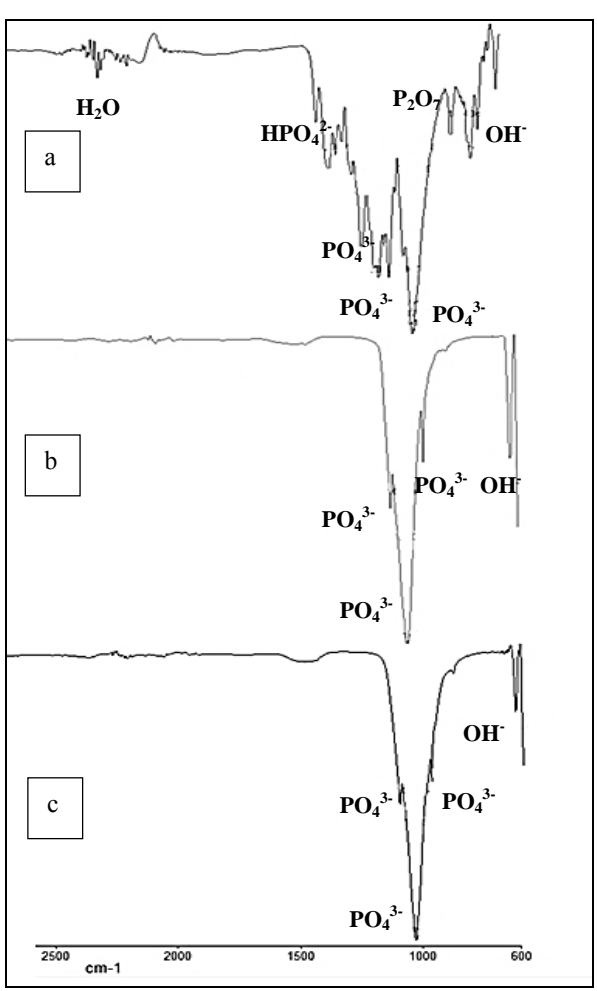


Figure 1 : FTIR spectra of HAP prepared for Ca/P ratio of (a) 0.67 (b) 1.67 and (c) 2.67

Phosphate groups (PO₄³⁻) asymmetric stretching vibration synthesized detected at wave number 1019 cm⁻¹ which indicates that the crystals formed in the synthesis results. In addition, the hydroxyapatite visible spectrum characteristic absorption band around 2021 cm H₂O⁻¹, 2167 cm⁻¹ and 2182 cm⁻¹. An increase in the intensity of the band 2250-2000 cm⁻¹ which is a band of H₂O on the surface because the surface absorbs water samples HAP. This is possible because the sample storage techniques unfavorable silica gel which does not include the storage time or may also be due to HAP produced from the calcination process becomes more hygroscopic due to the higher calcination temperature. The measurement results of hydroxyapatite synthesized using low temperature hydrothermal method with 2.67 Ca/P ratio using FTIR analysis shown in Figure 2. Phosphate

groups (PO_4^{3-}) asymmetric stretching vibration synthesized detected at wave number $1024~\rm cm^{-1}$ and $1085~\rm cm^{-1}$ which indicates that the crystals formed in the synthesis results. In addition, the hydroxyapatite visible spectrum characteristic of the OH absorption band around 3642 cm⁻¹. This can happen because the HAP powder is hygroscopic, thus precipitating the hydration of the air. OH group at 3642 cm⁻¹ region is called water absorption. Ribbon uptake carbonate (CO_3^{2-}) synthesis were also detected at wave number $1423~\rm cm^{-1}$ which is the asymmetric stretching vibration absorption band is weak with no form of symmetry.

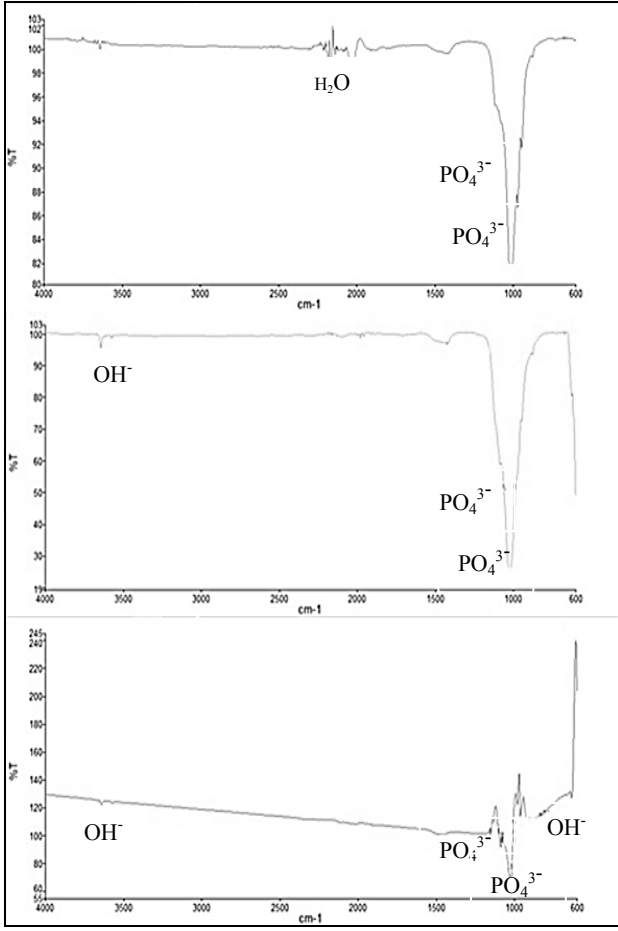


Figure 2 : FTIR spectra of HAP prepared at reaction temperature of (a) 70°C (b) 80°C and (c) 90°C

The measurement results of hydroxyapatite synthesized using hydrothermal method with low temperature of 90°C using FTIR analysis shown in Figure 2. Phosphate groups (PO₄³⁻) asymmetric stretching vibration synthesized detected at wave number 1025 cm⁻¹ and 1241 cm⁻¹ which indicates that the crystals formed in the synthesis results. Ribbon phosphate present in the spectrum of commercial hydroxyapatite as a small band at wave number 878 cm⁻¹, 961 cm⁻¹ and 981 cm⁻¹. In addition, the hydroxyapatite visible spectrum characteristic of the OH⁻

absorption band around 3641 cm⁻¹ and 636 cm⁻¹. This can happen because the HAP powder is hygroscopic, thus precipitating the hydration of the air. OH group at 3641 cm⁻¹ region is called water absorption, whereas the OH groups were detected around the wave number of 636 cm⁻¹ is an illustration of the water absorption. Carbonate absorption band (CO₃²⁻) synthesis were also detected at wave number 1463 cm⁻¹ which is the asymmetric stretching vibration absorption band is weak with no form of symmetry.

3.2 X-ray Analysis

From the results of XRD analysis, it is found that a change in the intensity of the peak from diffractogram. The results of XRD analysis as shown in Figure 3 where for each sample shows the majority present of peaks are hydroxyapatite. Peak of the hydroxyapatite 0.67 Ca/P ratio sample at 20 25.853°, 31.719° and 32.847° with hkl (002), (211) and (300). In the 1.67 Ca/P ratio sample at 20 25.853°, 31.740°, and 32.857° with hkl (002), (211) and (300). And on the 2.67 Ca/P ratio sample at 20 25.879°, 31.739°, and 32.865° with hkl (002), (211) and (300). Where in the peak hkl values are similar to pattern characterization results of XRD analysis from JCPDS (Joint Committee on Powder Diffraction Standards) with PDF Card No. 09-432. In addition, from the data base of results obtained XRD analysis of crystal crystal diameter each sample based on the Scherrer equation, where the crystal diameter grew along with the increasing ratio of Ca/P and temperature is shown in table 1.

Table 1: The average crystallite size of the samples

Ca/P ratio	Reaction temperature (°C)	Crystal diameter (nm)
0.67	90	54.38
1.67	90	52.37
2.67	90	52.32
2.67	70	63.43
2.67	80	55.85
2.67	90	52.48

Based on the analysis of XRD peaks can also be seen other than hydroxyapatite on samples where each sample contains phases as shown in Table 2. In samples with a ratio of 0.67 there is a phase other than the phase composition of hydroxyapatite, the calcium pyrophosphate. The calcium pyrophosphate compound formed by calcium hydroxide derived from the mixing of CaO with water reacts with phosphoric acid, resulting in a calcium dihydrogen phosphate as the following equation:

$$Ca(OH)_2 + 2H_3PO_4 \longrightarrow Ca(H_2PO_4)_2 + 2H_2O$$
 (3)

Then calcium dihydrogen phosphate reacts with ammonia to produce monetite (CaHPO4) or dicalcium phosphate anhydrous (DCPA) as shown in the following reaction:

$$Ca(H_2PO_4)_2 + NH_3 \longrightarrow CaHPO_4 + NH_4H_2PO_4$$
 (4)

Table 2: Phase contained in different Ca/P ratio samples

	-	-		-	 			_	-	-	_		 	-	 	-1	-	
	C	a/P	rat	io														

	Mineral phase
0.67	Hydroxiapatite, Calcium phosphate
1.67	Hydroxiapatite, Tricalcium phosphate
2.67	Hydroxiapatite, Calcium hydroxide

Where monetite (DCPA) is what causes the formation of calcium pyrophosphate. Monetite (DCPA) decomposes into calcium pyrophosphate at a temperature of 700-900°C, this was also a study done by Alqap and Sopyan [9].

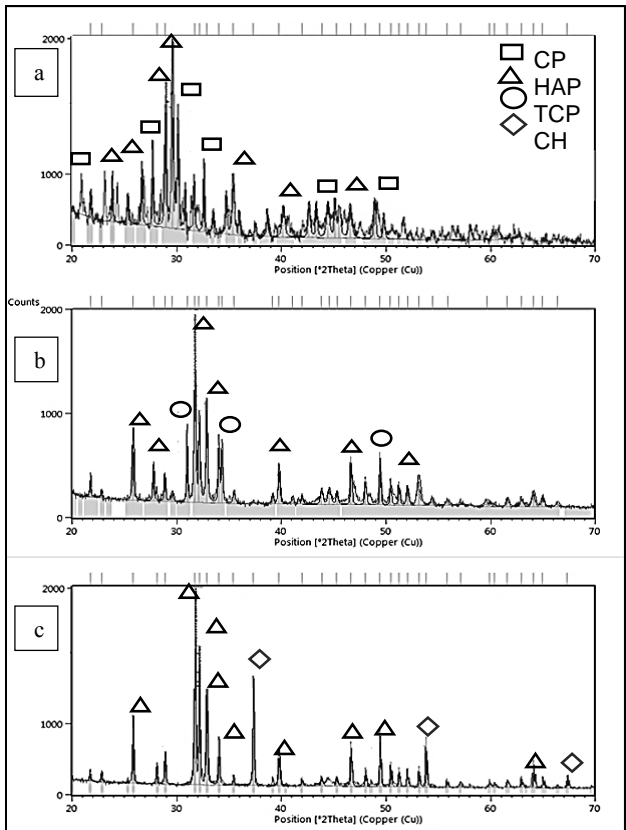


Figure 3 : XRD patterns of HAP at Ca/P ratio of (a) 0,67 (b) 1,67 and (c) 2,67

In samples with a ratio of 1.67 Ca/P phase composition consisting of hydroxyapatite, and tricalcium phosphate. The formation of tricalcium phosphate in 0.67 Ca/P sample is influenced by the ratio of Ca/P in which the ratio of Ca/P is smaller than tricalcium phosphate hydroxyapatite, it is also consistent with studies conducted by Zhang and Darvell [13] where tricalcium phosphate formed in the mass ratio of Ca/P 1.67. Also according Alqap and Sopyan [9] CaO were still present in the sample can cause the formation of tricalcium phosphate and calcium pyrophosphate react like the following reaction:

$$Ca_2P_2O_7 + CaO \longrightarrow Ca_3(PO_4)_2$$
 (5)

While the 2.67 Ca/P sample phase composition was consisting of hydroxyapatite and calcium hydroxide. Where calcium hydroxide CaO derived from mixing with water following reaction:

$$CaO + H_2O \longrightarrow Ca(OH)_2$$
 (6)

3.2 Morphology Sample

From the results of SEM morphology appears apatite crystals that gather several compounds that appear larger with a smooth and uniform grain [14]. Samples with higher heating temperatures produce crystals with a purity higher than samples with lower heating temperatures. Because of the high temperature heating will make the process of better particles growth [15].

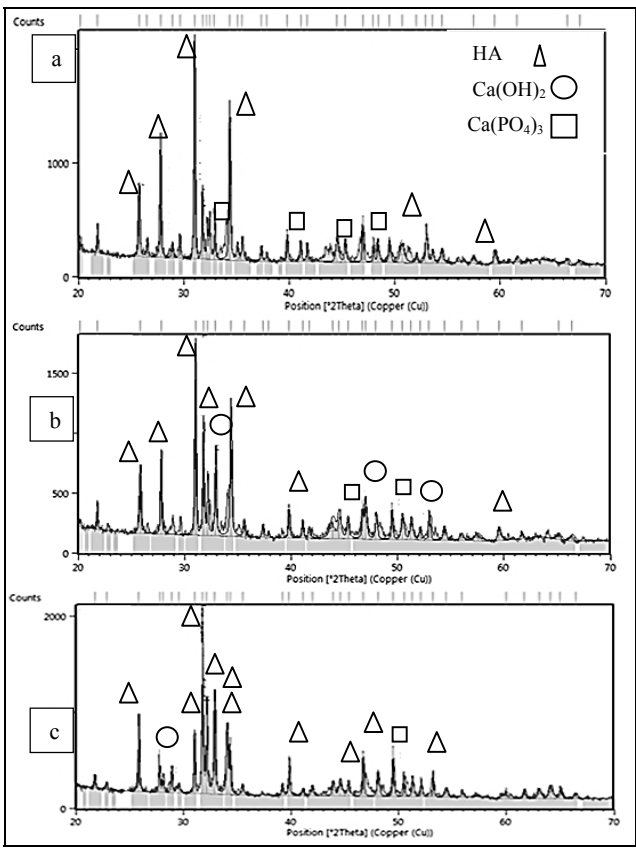


Figure 4 : FTIR spectra of HAP at reaction temperature of (a) 70°C (b) 80°C and (c) 90°C

The sample has a monoclinic and hexagonal crystalline structure. A monoclinic crystalline structure that has an axis that is tilted from its three axes. A axis perpendicular to the axis b; b perpendicular to c, but not c-axis perpendicular to the axis a. All three axes are unequal in length, generally the longest c axis and the shortest axis b. While a hexagonal crystalline structure that has 4 axes of symmetry with the symmetry axis lies in the 3 1

field, which is horizontal. The third axis of symmetry makes an angle of 60° between the horizontal axis and the fourth axis is the vertical axis is cut perpendicular to the axis of symmetry horizontal third. The fourth axis is usually longer than the third horizontal axis. Results of SEM for the results of the synthesis of hydroxyapatite with reaction temperature of 70°C, 80°C and 90°C is shown in Figure 5.

Samples with the SEM observation results using 7500x magnification can be seen in Figure 5. The results of observation samples with reaction temperature of 70°C, 80°C and 90°C (Figure 5) looks like a group of small dense particles. Grain size of the 90°C reaction temperature sample looks smaller than the 70°C and 80°C samples. This is reinforced by the results of the calculation of the size of the crystals from the XRD pattern. Defined as an individual crystal grains. The size of the crystal sample is 63.43 nm where as 70°C reaction temperature sample, 80°C and 90°C samples are 52.85 nm and 52.48 nm. The increase in temperature resulted in an increased thermal vibration energy, which then accelerates the diffusion of atoms through the grain boundaries, small droplets into larger ones. From Figure 5 it can be seen that the distance between the particles are initially very tight show tenuous when the heating temperature is lower.

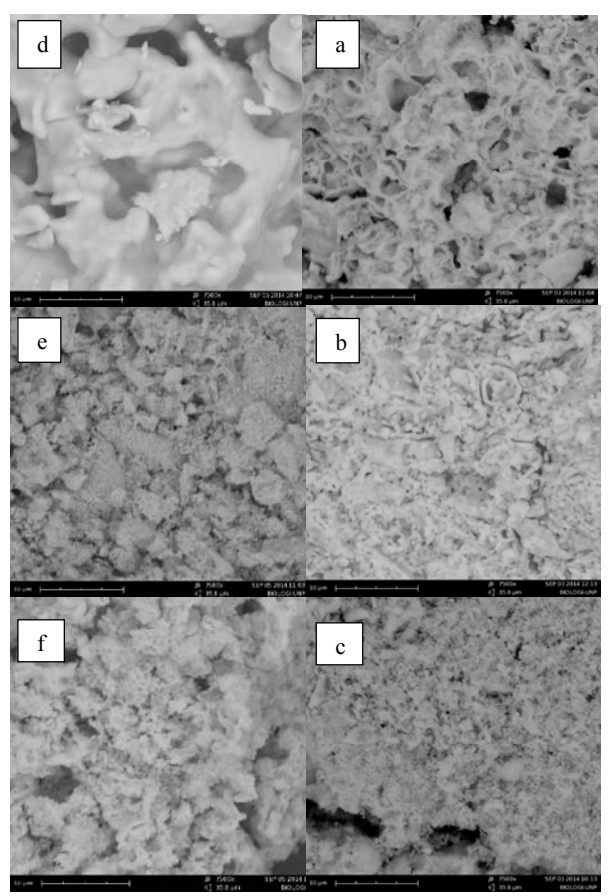


Figure 5: SEM results for sample with reaction temperature of (a) 70°C (b) 80°C, (c) 90°C and Ca/P ratio of (a) 0,67 (e) 1,67 (f) 2.67

Figure 5 shows the results of the samples with variation of the ratio Ca/P.In sample with the Ca/P ratio of 0.67 is shown in Figure 5 d has a larger size than the other samples (1.67 and 2.67 Ca/P ratio samples), this is caused by the presence of some other apatite compounds contained in the sample as has been seen in the results of XRD and FTIR analysis. SEM results also showed that the synthesis of the ratio of Ca/P of 0.67 in both immature hydroxyapatite. SEM result for sample with the ratio Ca/P of 1.67 is shown in Figure 5 e. From the results of SEM photograph looks morphology with finer grains. It is also caused by the presence of other compounds such as tricalcium phosphate apatite were also seen in the results of XRD analysis. For sample with the ratio Ca/P of 2.67 is shown in Figure 5 f. From the results of SEM morphology of the grains appear smoother and more uniform compare to 0.67 and 1.67 Ca/P ratio samples. In accordance with the X-ray diffraction pattern showed that the synthesis of the ratio of 2.67 Ca/P ratio produce hydroxyapatite peaks more than 0.67 and 1.67 Ca/P ratio samples.

4.0 CONCLUSION

Effect of Ca/P ratio and reaction temperature on chemical properties of hydroxyapatite powder from sea shell using low temperature hydrothermal method has been presented the paper. The crystal diameter of HAP at Ca/P ratio of 0.67, 1.67 and 2.67 were 53.38, 52.37 and 52.32 respectively. HAP phase at Ca/P ratio of 2.67 and 90°C temperature reaction was found predominant.

ACKNOWLEDGEMENTS

The authors would like to convey a great appreciation to DIKTI for supporting this research through Hibah Kompetensi 2014..

REFERENCE

- Gosain, A. K., & Persing, J. A. (1999). Biomaterials in The Face: Benefits and Risks. Journal of Craniofacial Surgical 10: 404-14.
- Kuo, T. C., Lee B. S., Kang, S. H., Lin, F. H., & Lin, C. P. (2007). Cytotoxicity of DP-bioglass paste used for treatment of dentin hypersensitivity. Journal of Endodontics 33: 451-454.
- Hench, L. L. (1991). Bioceramics: from concept to clinic. Journal of The American Ceramic Society 74: 1487-510
- Mobasherpur, I., Heshajin, M. S., Kazemzadeh, A., & Zakeri, M. (2007). Synthesis of nanocrystalline hydroxyapatite by using precipitation method. Journal of Alloys and Compounds 430(1-2): 330-333.
- Fahami A., Ebrahimi-Kahrizsangi R., & Nasiri-Tabrizi, B. (2011). Mechanochemical synthesis of hydroxyapatite/titanium nanocomposite. Solid State Sciences 13: 135-141.
- Rhee, S.-H. (2002). Synthesis of hydroxyapatite via mechanochemical treatment. Biomaterials 23(4): 1147-1152.
- Sadat-Shojai, M., Khorasani, M.-T., & Jamshidi, A. (2012). Hydrothermal processing of hydroxyapatite nanoparticles—a taguchi experimental design approach. Journal of Crystal Growth 361: 73-84.
- 8. Zhang, X., & Vecchio, K. S. (2006). Creation of dense

-Science and Engineering-

- hydroxyapatite (synthetic bone) by hydrothermal conversion of seashells. Materials Science and Engineering C 26: 1445-1450
- Alqap A. S. F., & Sopyan, I. (2009). Low temperature hydrothermal synthesis of calcium phosphate ceramics: effect of excess Ca procursor on phase behaviour. Indian Journal of Chemistry 48: 1492-1500.
- Sadat-Shojai, M., Atai, M. & Nodehi, A. (2011). Design of experiments (DOE) for the optimization of hydrothermal synthesis of hydroxyapatite nanoparticles. Journal of Brazillian Chemical 22: 571-582.
- Zhang, X., Vecchio, K. S., Massie J. B., Wang m., & Kim, C. W. (2007). Conversion of bulk seashells to biocompatible hydroxyapatite for bone implants. Acta Biomaterialia 3: 910–918.
- Sopyan, I., Mel, M., Ramesh, S., & Khalid, K. A. (2007).
 Porous hydroxyapatite for artificial bone applications.
 Science and Technology of Advanced Materials 8: 116-123
- 13. Zhang, H., & Darvell, B. W. (2011). Morphology and structural characteristics of hydroxyapatite whiskers: effect of the initial Ca concentration, Ca/P ratio and pH. Acta Biomaterialia 7: 2960-2968.
- Wu, S.-C., Tsou, H.-K., Hsu, H.-C., & Liou, S.-P. (2013). A hydrothermal synthesis of eggshell and fruit waste extract to produce nanosized hydroxyapatite. Ceramics International 39: 8183-8188.
- 15. Moore, W. R., Graves, S. E. & Bain, G. I. 2001. Synthetic bone graft substitutes. ANZ Journal of Surgery 71: 354-361.